

Electronic Supporting Information:

"Pyrazolate-supported Cr₃(μ₃-O) cores; homovalent Cr^{III}₃ and mixed-valent Cr^{III}₂Cr^{IV}"

Jessica M. López-Plá, Mohammed Obies, Georgia Zahariou, Michael Pissas, Yiannis Sanakis, John E. McGrady and Raphael G. Raptis

	Page
Synthesis	2
Crystal Data	2
Figure S1. UV-vis-NIR spectra of 1 (blue trace) and 2 (red trace).	3
Figure S2. ¹ H-nmr spectrum of complex 1 ; 400 MHz, CD ₂ Cl ₂ .	4
Figure S3. Thermal ellipsoid (50% probability) diagram of the crystal structure of 2	4
Figure S4. Infrared spectra of compounds 1 (blue trace) and 2 (red trace).	5
Figure S5. VT-EPR spectra of a frozen CH ₂ Cl ₂ solution of 1 , recorded at the indicated temperatures. The spectra have been scaled as dI/dB × T. EPR conditions: Microwave frequency, 32 mW; modulation amplitude, 2.5 G _{pp} ; microwave frequency, 9.39 GHz.	5
Figure S6. Cyclic and differential pulse voltammograms of (Ph ₄ P) ₂ [Cr ₃ (μ ₃ -O)(μ-4-Cl-pz) ₃ Cl ₃] (1) (vs Fc ⁺ /Fc); 0.45 M Bu ₄ NPF ₆ /CH ₂ Cl ₂ , 150 mV/s sweep.	6
Figure S7. Cyclic voltammogram of (Ph ₄ P) ₂ [Cr ₃ (μ ₃ -O)(μ-4-Cl-pz) ₃ Br ₃] (2) (vs Fc ⁺ /Fc); 0.45 M Bu ₄ NPF ₆ /CH ₂ Cl ₂ , 150 mV/s sweep.	6
Computational methods	7
Table S1. Average X-ray values, computed structure parameters (bond lengths in Å), and Mulliken spin density (ρ) for [Cr ₃ Cl ₃] ²⁻ and [Cr ₃ Cl ₃] ¹⁻ . All calculations were done with the PBE functional.	7
Table S2. Optimised cartesian coordinates (PBE)	8
Figure S8. Experimental and TD-DFT spectra using the CAM-B3LYP functional (compare Figure 3 of the main text for the B3LYP version).	9
Figure S9. Natural orbitals of CAS(9,9) active space of 1 ²⁻ .	10
Table S3. wavefunction compassions and weight for the five multiplicities.	11
Figure S10. Op orbitals of the CAS(15,12) active space of the 1 ²⁻ molecule.	12
Table S5. NEV-PT2 energy and relative energies of different spin multiplicities of 1 ²⁻ and 1 ¹⁻ molecules.	12

Synthesis: $(\text{Ph}_4\text{P})_2[\text{Cr}_3(\mu_3-\text{O})(\mu\text{-4-Cl-pz})_3\text{Cl}_3]$ (**1**): A reaction mixture of $\text{Cr}(\text{NO}_3)_3 \cdot 9\text{H}_2\text{O}$ (24 mg, 0.59 mmol), 4-Cl-pzH (18 mg, 1.78 mmol) and NEt_3 (200 μL , 1.47 mmol) in 10 mL butyronitrile was heated to 373 K for 1 h. To the resulting pink solution, was added Ph_4PCl (45 mg, 1.18 mmol) and heating continued for 0.5 h. The solvent was removed under vacuum and the pink solid product was washed with EtOH and Et_2O and recrystallized from $\text{CH}_2\text{Cl}_2/\text{Et}_2\text{O}$ (48 mg of X-ray quality crystalline product, 5%). For **1**: Calc. (Found) C, 48.74 (48.82); H, 3.30 (3.40); N, 10.18 (10.08); $^1\text{H-NMR}$ (400 MHz, CD_2Cl_2 , ppm) 1.57 (s, 12 H, H^3/H^5), 7.59 (m, 80 H, Ph_4P^+); UV-Vis-NIR, CH_2Cl_2 , $\lambda_{\text{max}}/\text{cm}^{-1}(\varepsilon/\text{M}^{-1}\text{cm}^{-1})$ 27100(575), 23500(410), 18700 (190); IR (CsI, cm^{-1}) 3120w, 3062w, 1652w, 1586w, 1558w, 1484m, 1439s, 1389s, 1305s, 1229w, 1184s, 1170m, 1109s, 1035s, 994s, 964s, 841s, 760s, 723s, 689s, 617s, 529s, 445m.
 $(\text{Ph}_4\text{P})_2[\text{Cr}_3(\mu_3-\text{O})(\mu\text{-4-Cl-pz})_3\text{Br}_3]$ (**2**): A reaction mixture of $\text{Cr}(\text{NO}_3)_3 \cdot 9\text{H}_2\text{O}$ (20 mg, 0.50 mmol), 4-Cl-pzH (15 mg, 1.51 mmol) and NEt_3 (175 μL , 1.26 mmol) in 10 mL butyronitrile was heated to 373 K for 1 h. To the resulting pink solution, was added Ph_4PBr (42 mg, 1.00 mmol) and heating continued for 0.5 h. The solvent was removed under vacuum and the pink solid product was washed with EtOH and Et_2O and recrystallized from $\text{CH}_2\text{Cl}_2/\text{Et}_2\text{O}$ (52 mg of X-ray quality crystalline product, 6%). For **2**: Calc. (Found) C, 45.10(44.88); H, 3.05 (3.14); N, 9.42 (9.73); $^1\text{H-NMR}$ (400 MHz, CD_2Cl_2 , ppm) 1.81 (s, 12 H, H^3/H^5), 7.63 (m, 80 H, Ph_4P^+); UV-Vis-NIR, CH_2Cl_2 , $\lambda_{\text{max}}/\text{cm}^{-1}(\varepsilon/\text{M}^{-1}\text{cm}^{-1})$ 28900(500), 24800(400), 19570 (150); IR (CsI, cm^{-1}) 3120w, 3062w, 1652w, 1586w, 1558w, 1484m, 1439s, 1389s, 1305s, 1229w, 1194s, 1170m, 1109s, 1040s, 998s, 985s, 841s, 760s, 723s, 689s, 617s, 529s.

Crystal data: for **1**: $(\text{Ph}_4\text{P})_2[\text{Cr}_3(\mu_3-\text{O})(\mu\text{-4-Cl-pz})_3\text{Cl}_3] \cdot \text{CH}_2\text{Cl}_2$: $\text{C}_{67}\text{H}_{54}\text{Cl}_{11}\text{Cr}_3\text{N}_{12}\text{OP}_2$, Mr = 1650.10, orthorhombic, space group $Pna2_1$, $a = 23.746(5)$, $b = 17.540(4)$, $c = 16.981(4)$ Å, $V = 7073(3)$ Å 3 , $Z = 4$, T = 100 K, 96314 reflections ($R_{\text{int}} = 0.171$), 12054 unique, $R_1 = 0.0713$, $wR_2 = 0.1491$, GoF = 1.058 for 8249 observed reflections [$|I| > 2\sigma(I)$] and 866 parameters (CCDC 2358560). Crystal data: for **2**: $(\text{Ph}_4\text{P})_2[\text{Cr}_3(\mu_3-\text{O})(\mu\text{-4-Cl-pz})_3\text{Br}_3] \cdot \text{CH}_2\text{Cl}_2$: $\text{C}_{67}\text{H}_{54}\text{Br}_3\text{Cl}_8\text{Cr}_3\text{N}_{12}\text{OP}_2$, Mr = 1784.49, orthorhombic, space group $Pna2_1$, $a = 24.0399(10)$, $b = 17.8794(8)$, $c = 16.9017(7)$ Å, $V = 7264.7(5)$ Å 3 , $Z = 4$, T = 150 K, 160232 reflections ($R_{\text{int}} = 0.090$), 14916 unique, $R_1 = 0.0472$, $wR_2 = 0.1035$, GoF = 1.046 for 12071 observed reflections [$|I| > 2\sigma(I)$] and 866 parameters (1 restraint) (CCDC 2358561).

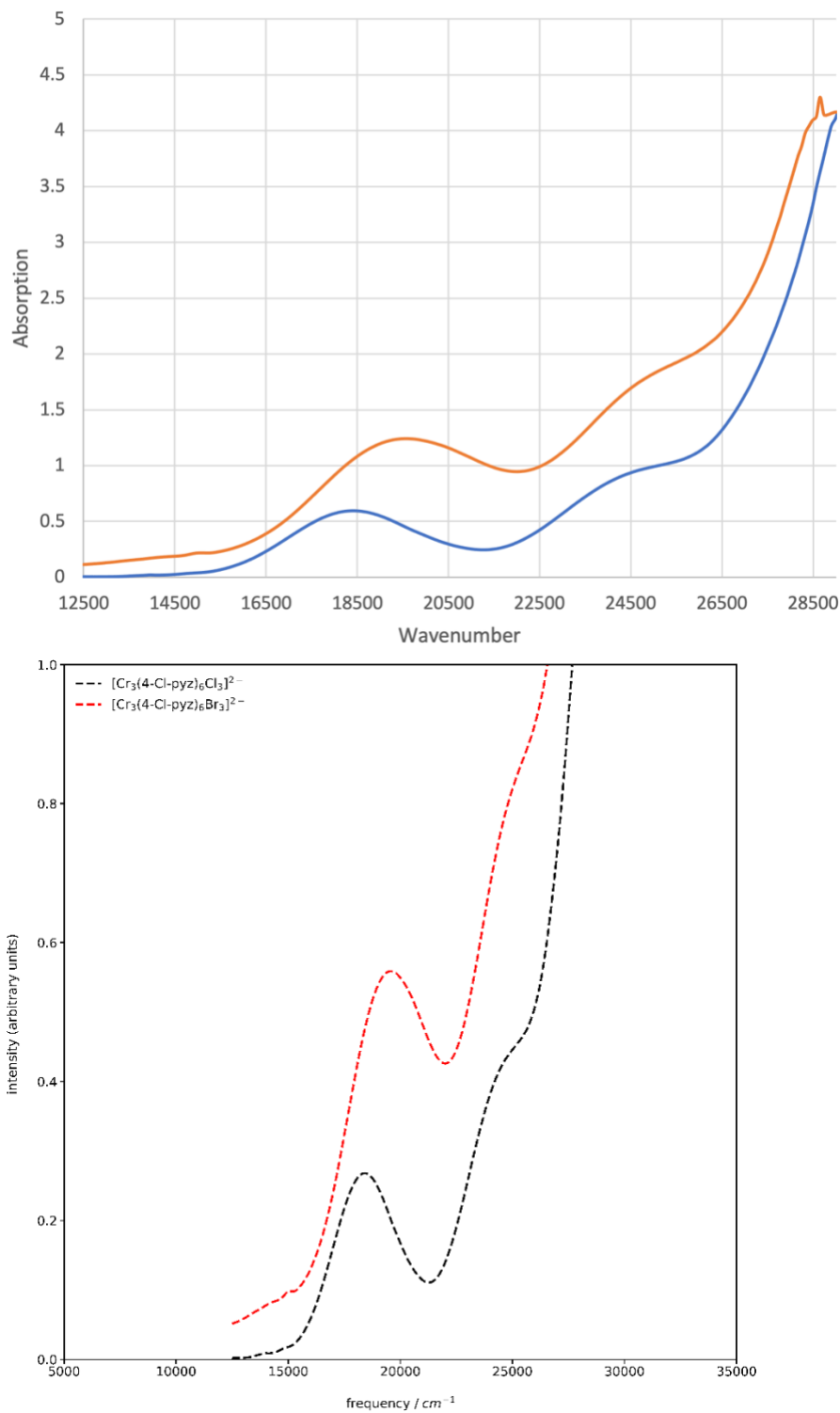


Figure S1. UV-vis-NIR spectra of **1** (blue trace) and **2** (red trace).

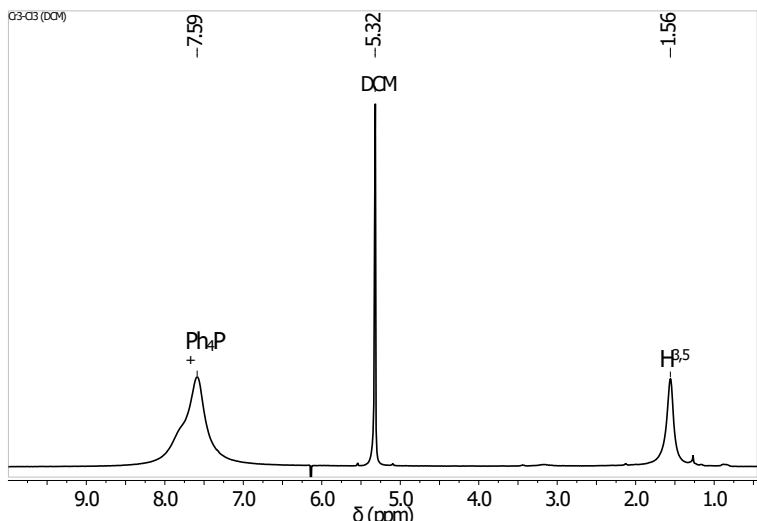


Figure S2. ¹H-nmr spectrum of complex **1**; 400 MHz, CD₂Cl₂.

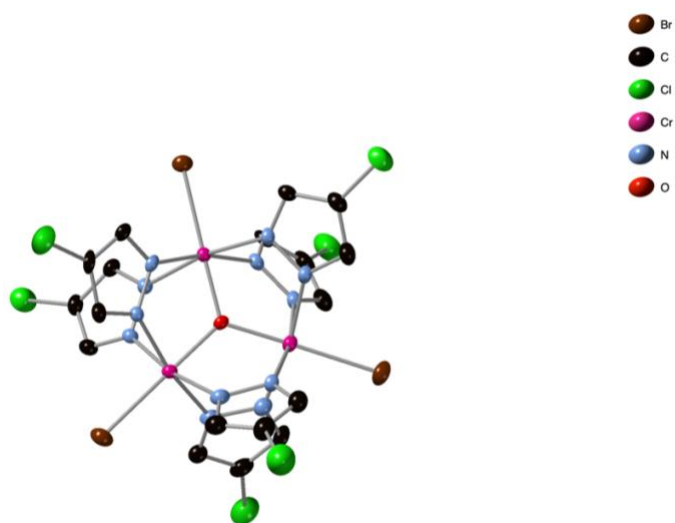


Figure S3. Thermal ellipsoid (50% probability) diagram of the crystal structure of **2** (hydrogen atoms not shown).

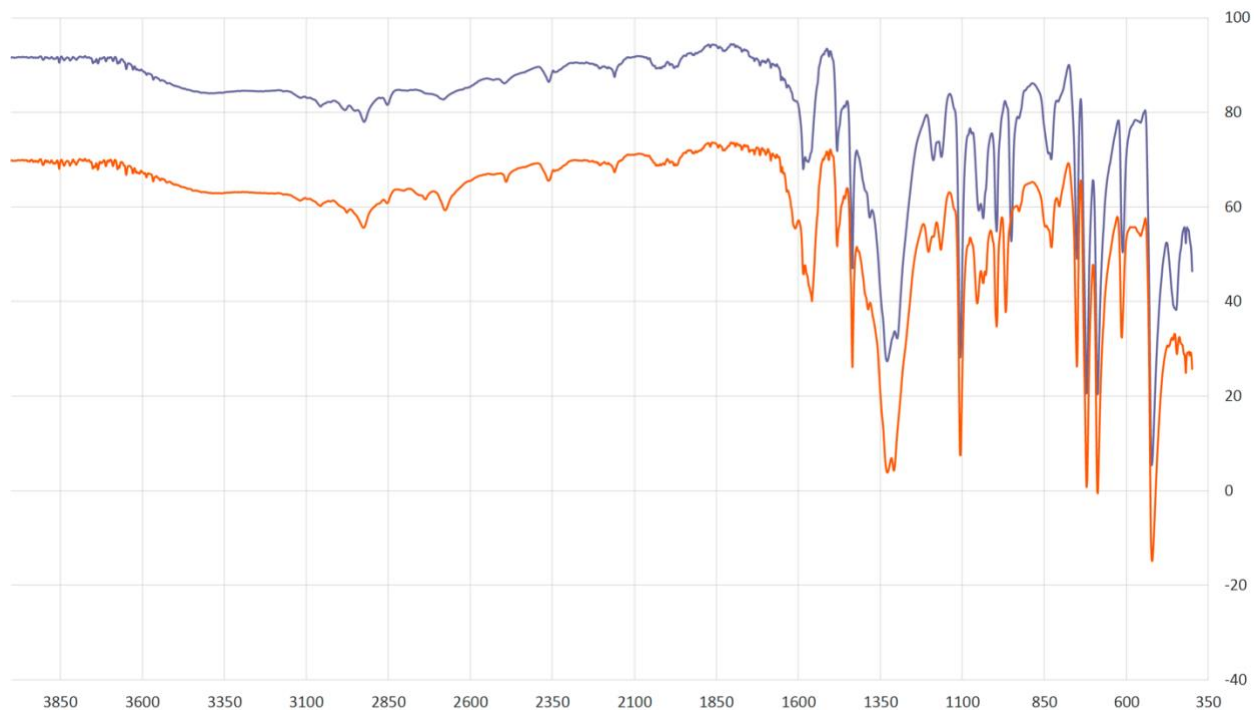
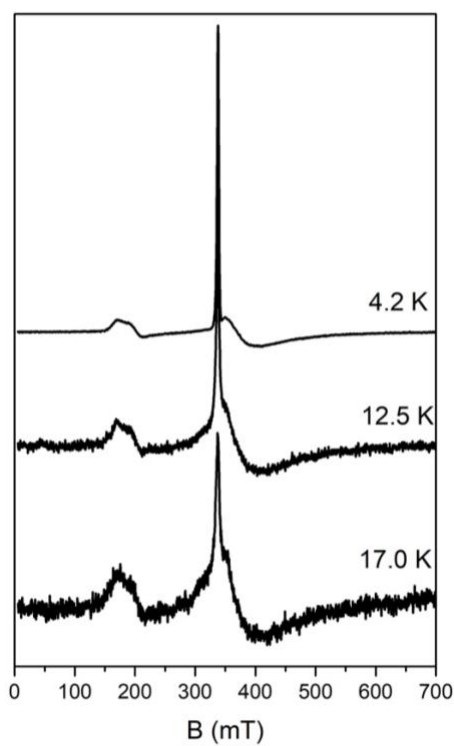


Figure S4. Infrared spectra of compounds **1** (blue trace) and **2** (red trace).



S5. VT-EPR spectra of a frozen CH₂Cl₂ solution of **1**, recorded at the indicated temperatures. The spectra have been scaled as dI/dB × T. EPR conditions: Microwave frequency, 32 mW; modulation amplitude, 2.5 G_{pp}; microwave frequency, 9.39 GHz.

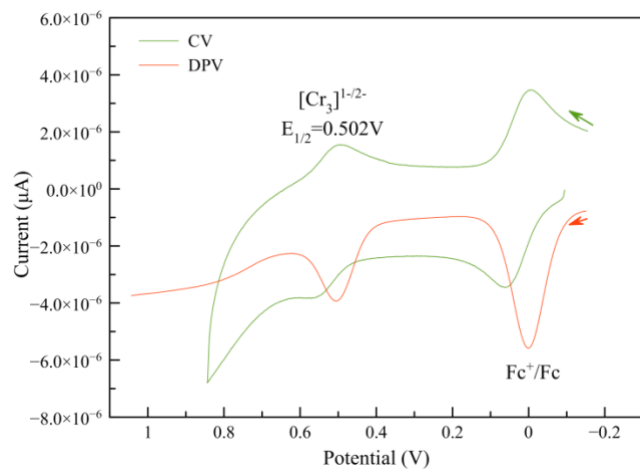
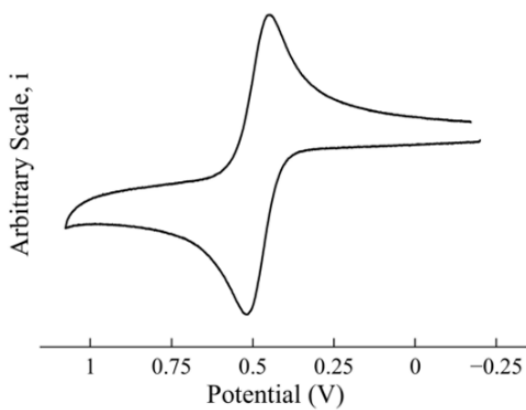


Figure S6. Cyclic and differential pulse voltammograms of $(\text{Ph}_4\text{P})_2[\text{Cr}_3(\mu_3\text{-O})(\mu\text{-4-Cl-pz})_3\text{Cl}_3]$ (**1**) (vs Fc^+/Fc); 0.45 M $\text{Bu}_4\text{NPF}_6/\text{CH}_2\text{Cl}_2$, 150 mV/s sweep.

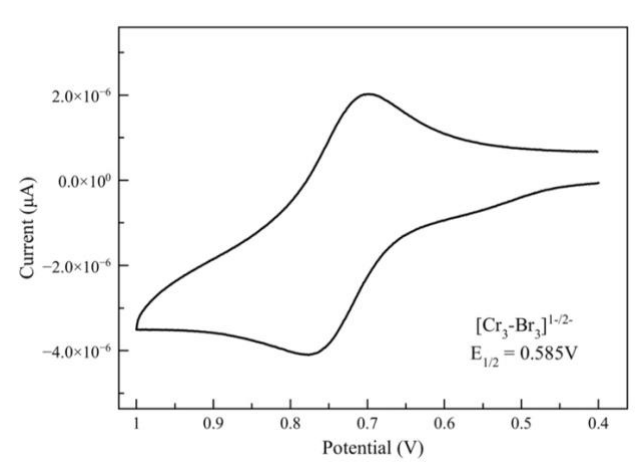


Figure S7. Cyclic voltammogram of $(\text{Ph}_4\text{P})_2[\text{Cr}_3(\mu_3\text{-O})(\mu\text{-4-Cl-pz})_3\text{Br}_3]$ (**2**) (vs Fc^+/Fc); 0.45 M $\text{Bu}_4\text{NPF}_6/\text{CH}_2\text{Cl}_2$, 150 mV/s sweep.

Electronic structure of $[\text{Cr}_3(4\text{-Cl-pz})_6\text{Cl}_3]^{2-}$ and $[\text{Cr}_3(4\text{-Cl-pz})_6\text{Cl}_3]^{1-}$, $\mathbf{1}^{2-}$ and $\mathbf{1}^{1-}$

Computational methods

All calculations in this paper were performed using the ORCA suite of quantum chemical programmes, version 5.0.3.^{1,2} Density functional theory (DFT) was used to perform the structural optimisations with the PBE functional,³ a def2-TZVP basis⁴ with the associated pseudopotentials⁵ on Cr, Cl/Br, O and N and a def2-SVP basis on C and H. A continuum model was used to replicate the effects of the CH_2Cl_2 solvent. Time-dependent density functional theory (TD-DFT) performed using the Tamm-Dancoff approximation⁶ and a range of functionals including PBE, B3LYP⁷ and the range-separated CAM-B3LYP,⁸ with the same solvent model. The RI approximation was used with the def2/J auxiliary basis set,⁹ and for hybrid functionals (B3LYP, CAM-B3LYP), the RIJCOSX approximation was used.¹⁰ For the CASSCF and NEVPT2 calculations, the def2-TZVP basis set was used on Cr and a def2-SVP basis on the rest of the atoms with AutoAux auxiliary basis set.^{11,12} The RIJCOSX approximation was used. Details of the selected active spaces are given below.

1- Optimised geometries of $\mathbf{1}^{2-}$ and $\mathbf{1}^{1-}$

Table S1 and Table S2 show the relative energies, Mulliken spin densities, optimised structural parameters and X-ray data for $\mathbf{1}^{2-}$ and $\mathbf{1}^{1-}$.

Table S1: Average X-ray values, computed structure parameters (bond lengths in Å), and Mulliken spin density (ρ) for $[\text{Cr}_3\text{Cl}_3]^{2-}$ and $[\text{Cr}_3\text{Cl}_3]^{1-}$. All calculations were done with the PBE functional.

	Cr—Cr	Cr—N	Cr—Cl	Cr—O	ρ_{Cr_1}	ρ_{Cr_2}	ρ_{Cr_3}
$[\text{Cr}_3(4\text{-Cl-pz})_6\text{Cl}_3]^{2-}$							
X-ray	3.21	2.06	2.32	1.86			
S = 9/2	3.24	2.08	2.35	1.87	3.21	3.21	3.21
$[\text{Cr}_3(4\text{-Cl-pz})_6\text{Br}_3]^{2-}$							
X-ray							
S = 9/2	3.24	2.08	2.53	1.87	3.23	3.23	3.23
$[\text{Cr}_3(4\text{-Cl-pz})_6\text{Cl}_3]^{1-}$							
S = 8/2	3.20	2.06	2.28	1.85	2.92	2.92	2.92

Optimised cartesian coordinates for the three complexes are collected in Table S2, below.

Table S2. Optimised cartesian coordinates (PBE)

$[\text{Cr}_3(4\text{-Cl-pz})_6\text{Cl}_3]^{2-}$	$[\text{Cr}_3(4\text{-Cl-pz})_6\text{Br}_3]^{2-}$	$[\text{Cr}_3(4\text{-Cl-pz})_6\text{Cl}_3]^{1-}$
O 0.0000 0.0000 -0.0002 Cr 0.0000 -1.6231 -0.9350 Cr -0.0000 0.0000 1.8721 Cr -0.0000 1.6231 -0.9350 Cl 0.0000 3.6588 -2.1118 Cl -0.0000 0.0000 4.2226 Cl 0.0000 -3.6588 -2.1118 N 1.4126 -1.5115 1.6606 C 2.3573 -2.0356 2.4688 C 2.9897 -3.0885 1.7853 C 2.3564 -3.1564 0.5324 N 1.4122 -2.1940 0.4811 H 2.5249 -1.6406 3.4759 H 2.5231 -3.8329 -0.3118 N -1.4126 -1.5115 1.6606 C -2.3573 -2.0356 2.4688 C -2.9897 -3.0885 1.7853 C -2.3564 -3.1564 0.5324 N -1.4122 -2.1940 0.4811 H -2.5249 -1.6406 3.4759 H -2.5231 -3.8329 -0.3118 N 1.4126 1.5115 1.6606 C 2.3573 2.0356 2.4688 C 2.9897 3.0885 1.7853 C 2.3564 3.1564 0.5324 N 1.4122 2.1940 0.4811 H 2.5249 1.6406 3.4759 H 2.5231 3.8329 -0.3118 N -1.4126 1.5115 1.6606 C -2.3573 2.0356 2.4688 C -2.9897 3.0885 1.7853 C -2.3564 3.1564 0.5324 N -1.4122 2.1940 0.4811 H -2.5249 1.6406 3.4759 H -2.5231 3.8329 -0.3118 N 1.4101 0.6814 -2.1397 C 2.3525 1.1187 -3.0005 C 2.9839 0.0000 -3.5711 C 2.3525 -1.1187 -3.0005 N 1.4101 -0.6814 -2.1397 C -2.3525 1.1187 -3.0005 C -2.9839 0.0000 -3.5711 C -2.3525 -1.1187 -3.0005 N -1.4101 -0.6814 -2.1397 H -2.5188 2.1882 -3.1638 H -2.5188 -2.1882 -3.1638 N -1.4101 0.6814 -2.1397 C -2.3525 1.1187 -3.0005 C -2.9839 0.0000 -3.5711 C -2.3525 -1.1187 -3.0005 N -1.4101 -0.6814 -2.1397 H -2.5188 2.1882 -3.1638 H -2.5188 -2.1882 -3.1638 Cl 4.2678 0.0000 -4.7298 Cl 4.2764 -4.0888 2.3636 Cl -4.2764 -4.0888 2.3636 Cl -4.2678 0.0000 -4.7298 Cl -4.2764 4.0888 2.3636 Cl 4.2764 4.0888 2.3636	O -0.0000 -0.0000 0.0000 Cr -0.0000 -1.6211 -0.9339 Cr -0.0000 -0.0000 1.8700 Cr -0.0000 1.6211 -0.9339 N 1.4136 -1.5102 1.6598 C 2.3696 -2.0240 2.4620 C 3.0092 -3.0696 1.7746 C 2.3694 -3.1444 0.5256 N 1.4136 -2.1928 0.4799 H 2.5372 -1.6275 3.4685 H 2.5373 -3.8197 -0.3194 N -1.4136 -1.5102 1.6598 C -2.3696 -2.0240 2.4620 C -3.0092 -3.0696 1.7746 C -2.3694 3.1444 0.5256 N 1.4136 2.1928 0.4799 H 2.5372 -1.6275 3.4685 H 2.5373 3.8197 -0.3194 N 1.4136 1.5102 1.6598 C 2.3696 2.0240 2.4620 C 3.0092 3.0696 1.7746 C 2.3694 3.1444 0.5256 N 1.4136 2.1928 0.4799 H 2.5372 1.6275 3.4685 H 2.5373 3.8197 -0.3194 N 1.4109 0.6816 -2.1376 C 2.3643 1.1186 -2.9869 C 3.0022 -0.0000 -3.5499 C 2.3643 -1.1186 -2.9869 N 1.4109 -0.6816 -2.1376 C 2.3643 1.1186 -2.9869 C 3.0022 0.0000 -3.5499 C 2.3643 -1.1186 -2.9869 N 1.4109 -0.6816 -2.1376 H 2.5304 2.1884 -3.1487 H 2.5304 -2.1884 -3.1487 Cl 4.2986 -0.0000 -4.6933 Cl 4.3092 -4.0559 2.3449 Cl -4.3092 -4.0559 2.3449 Cl -4.2986 0.0000 -4.6933 Cl 4.3092 4.0559 2.3449 Cl 4.3092 4.0559 2.3449 Br -0.0000 0.0000 4.3967 Br -0.0000 -3.8076 -2.1983 Br -0.0000 3.8076 -2.1983	O 0.0000 -0.0000 -0.0007 Cr -0.0000 -1.6034 -0.9252 Cr 0.0000 0.0000 1.8482 Cr -0.0000 1.6034 -0.9252 Cl -0.0000 3.5761 -2.0662 Cl 0.0000 0.0000 4.1275 Cl -0.0000 -3.5761 -2.0662 N 1.4045 -1.4937 1.6484 C 2.3555 -2.0108 2.4530 C 2.9902 -3.0599 1.7663 C 2.3535 -3.1328 0.5156 N 1.4036 -2.1765 0.4689 H 2.5261 -1.6148 3.4589 H 2.5221 -3.8084 -0.3287 N -1.4045 -1.4937 1.6484 C -2.3555 -2.0108 2.4530 C -2.9902 -3.0599 1.7663 C -2.3535 -3.1328 0.5156 N -1.4036 -2.1765 0.4689 H -2.5261 -1.6148 3.4589 H -2.5221 -3.8084 -0.3287 N 1.4045 1.4937 1.6484 C 2.3555 2.0108 2.4530 C 2.9902 3.0599 1.7663 C 2.3535 3.1328 0.5156 N 1.4036 2.1765 0.4689 H 2.5261 1.6148 3.4589 H 2.5221 3.8084 -0.3287 N -1.4045 1.4937 1.6484 C -2.3555 2.0108 2.4530 C -2.9902 3.0599 1.7663 C -2.3535 3.1328 0.5156 N -1.4036 2.1765 0.4689 H -2.5261 1.6148 3.4589 H -2.5221 3.8084 -0.3287 N 1.4034 0.6814 -2.1184 C 2.3551 1.1194 -2.9678 C 2.9915 0.0000 -3.5308 C 2.3551 -1.1194 -2.9678 N 1.4034 -0.6814 -2.1184 H 2.5253 2.1885 -3.1289 H 2.5253 -2.1885 -3.1289 N -1.4034 0.6814 -2.1184 C -2.3551 1.1194 -2.9678 C -2.9915 0.0000 -3.5308 C -2.3551 -1.1194 -2.9678 N -1.4034 -0.6814 -2.1184 H -2.5253 2.1885 -3.1289 H -2.5253 -2.1885 -3.1289 Cl 4.2826 0.0000 -4.6733 Cl 4.2795 -4.0510 2.3387 Cl -4.2795 -4.0510 2.3387 Cl -4.2826 0.0000 -4.6733 Cl 4.2795 4.0510 2.3387 Cl 4.2795 4.0510 2.3387

2- TD-DFT calculations

TD-DFT calculations performed with the B3LYP functional are shown in Figure 4 in the main text. The corresponding data calculated using CAM-B3LYP are shown in Figure S8. The computed spectra of the dianions, **1**²⁻ and **2**²⁻, are very similar to those computed with B3LYP. The low-frequency CT band in **1-ox** is, however, blue shifted by 2000 cm⁻¹, affording a poorer match with experiment.

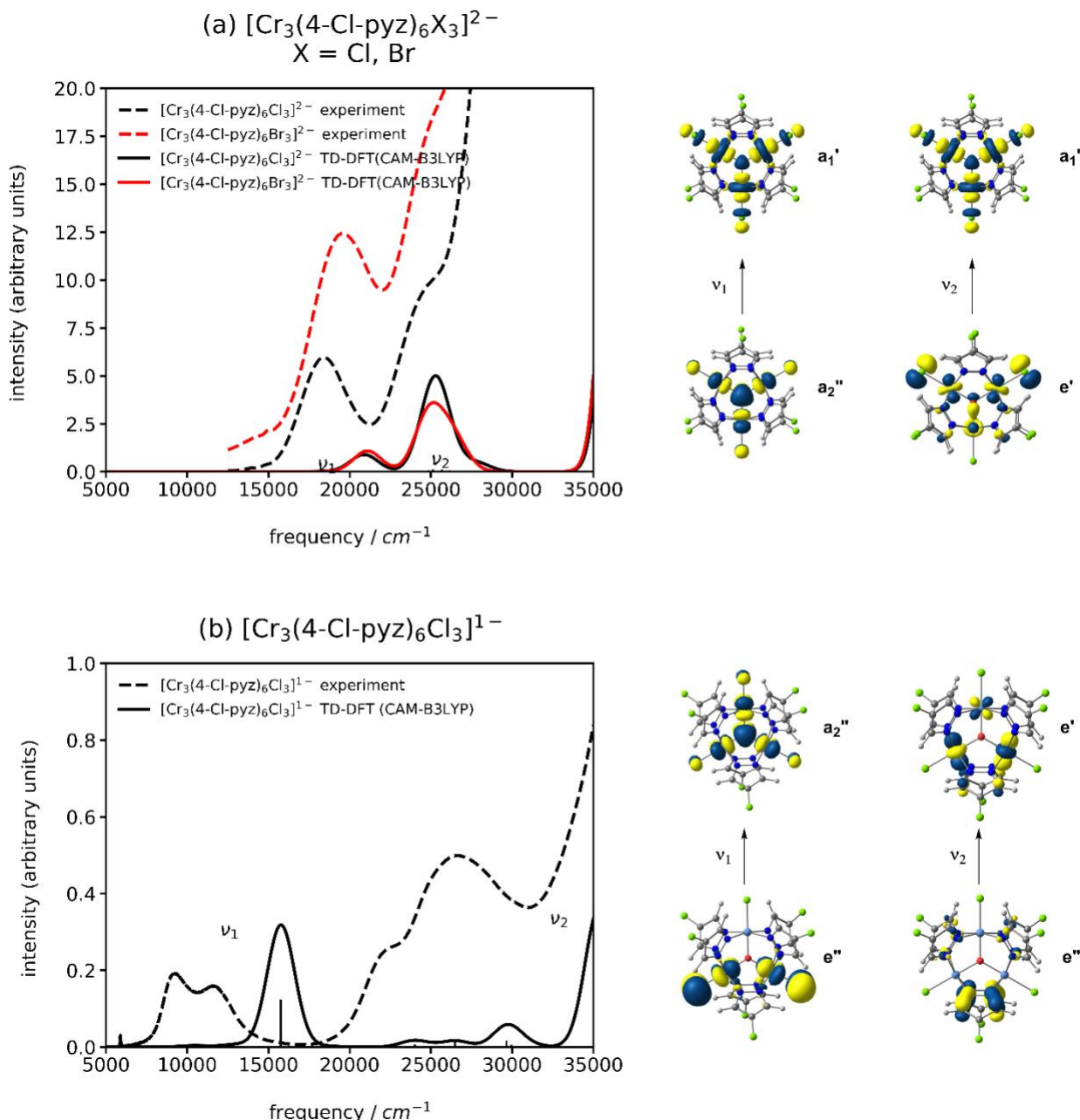


Figure S8. Experimental and TD-DFT spectra using the CAM-B3LYP functional (compare Figure 4 of the main text for the B3LYP version).

3- Multiconfigurational calculations on $\mathbf{1}^{2^-}$

In the single point CASSCF/NEVPT2 calculations on $\mathbf{1}^{2^-}$ we have adopted a CAS(9,9) active space, nine electrons in nine orbitals, using DFT-PBE optimized geometry. The nine correspond to the linear combinations of chromium d -based orbitals shown in Figure S9. The occupations number for states of different multiplicity are also shown in the Figure S9, and the weights of the high-weight configurations in the corresponding wavefunctions are shown in Table S4. The wavefunction of the $S = 9/2$ state contains only a single determinant, $\sigma^1 \sigma_{nb}^1 \sigma^{*1} \pi^1 \pi_{nb}^1 \pi^{*1} \delta^1 \delta_{nb}^1 \delta^{*1}$, and is therefore well described by DFT. The other four states, in contrast, are much more multiconfigurational in nature, and in the $S = 1/2$ state the first seven configurations make up only 10% of the total wavefunction. For the oxidized form ($\mathbf{1}^{1^-}$), a CAS(8,8) was adopted with DFT-PBE optimized geometry.

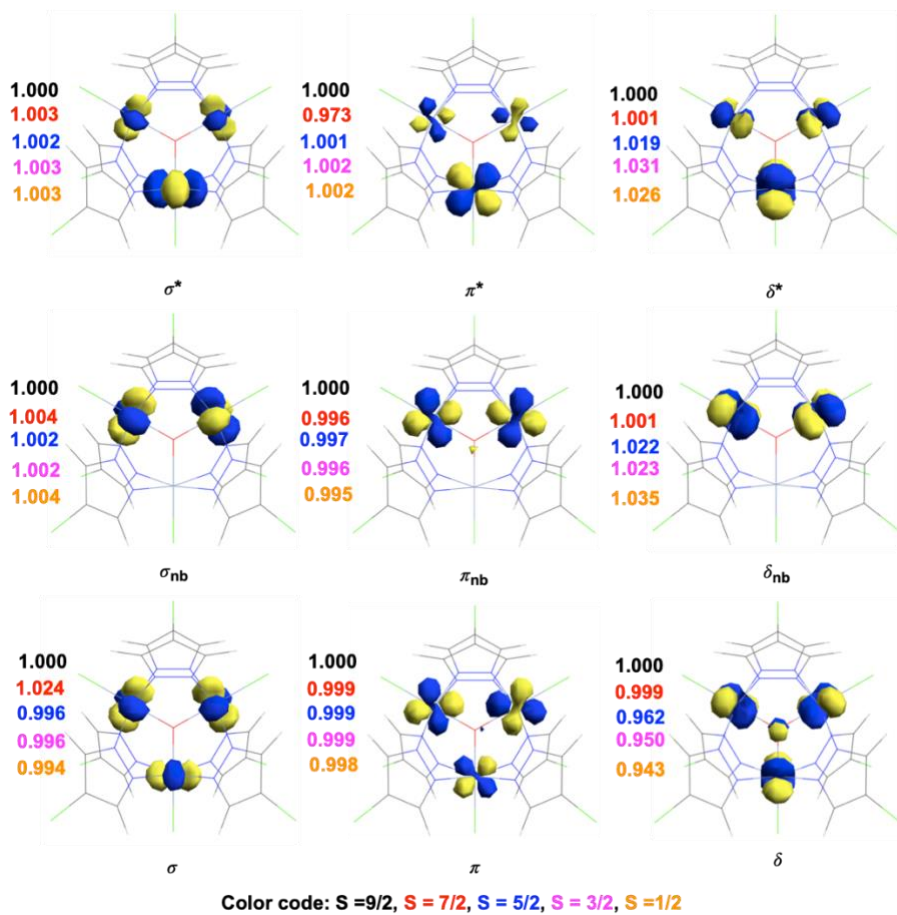


Figure S9. Natural orbitals of CAS(9,9) active space of $\mathbf{1}^{2^-}$.

Table S3. wavefunction compassions and weight for the five multiplicities

Multiplicity	Wavefunction	Weight %
S = 9/2	$\sigma^1 \sigma_{nb}^1 \sigma^{*1} \pi^1 \pi_{nb}^1 \pi^{*1} \delta^1 \delta_{nb}^1 \delta^{*1}$	100
S = 7/2	$\sigma^1 \sigma_{nb}^1 \sigma^{*1} \pi^1 \pi_{nb}^1 \pi^{*1} \delta^1 \delta_{nb}^1 \delta^{*1}$	17
	$\sigma^1 \sigma_{nb}^1 \sigma^{*1} \pi^1 \pi_{nb}^1 \pi^{*1} \delta^0 \delta_{nb}^1 \delta^{*2}$	17
	$\sigma^1 \sigma_{nb}^1 \sigma^{*1} \pi^1 \pi_{nb}^1 \pi^{*1} \delta^2 \delta_{nb}^1 \delta^{*0}$	17
	$\sigma^0 \sigma_{nb}^1 \sigma^{*2} \pi^1 \pi_{nb}^1 \pi^{*1} \delta^1 \delta_{nb}^1 \delta^{*1}$	14
	$\sigma^2 \sigma_{nb}^1 \sigma^{*0} \pi^1 \pi_{nb}^1 \pi^{*1} \delta^1 \delta_{nb}^1 \delta^{*1}$	5
	$\sigma^1 \sigma_{nb}^1 \sigma^{*1} \pi^0 \pi_{nb}^1 \pi^{*2} \delta^1 \delta_{nb}^1 \delta^{*1}$	5
	$\sigma^1 \sigma_{nb}^1 \sigma^{*2} \pi^1 \pi_{nb}^1 \pi^{*0} \delta^1 \delta_{nb}^1 \delta^{*1}$	4
	$\sigma^1 \sigma_{nb}^1 \sigma^{*1} \pi^1 \pi_{nb}^1 \pi^{*1} \delta^1 \delta_{nb}^1 \delta^{*1}$	5
S = 5/2	$\sigma^1 \sigma_{nb}^1 \sigma^{*1} \pi^1 \pi_{nb}^1 \pi^{*1} \delta^0 \delta_{nb}^1 \delta^{*2}$	5
	$\sigma^1 \sigma_{nb}^1 \sigma^{*1} \pi^1 \pi_{nb}^1 \pi^{*1} \delta^2 \delta_{nb}^1 \delta^{*0}$	5
	$\sigma^0 \sigma_{nb}^1 \sigma^{*2} \pi^1 \pi_{nb}^1 \pi^{*1} \delta^1 \delta_{nb}^1 \delta^{*1}$	5
	$\sigma^2 \sigma_{nb}^1 \sigma^{*0} \pi^1 \pi_{nb}^1 \pi^{*1} \delta^1 \delta_{nb}^1 \delta^{*1}$	4
	$\sigma^1 \sigma_{nb}^1 \sigma^{*1} \pi^0 \pi_{nb}^1 \pi^{*2} \delta^1 \delta_{nb}^1 \delta^{*1}$	4
	$\sigma^1 \sigma_{nb}^1 \sigma^{*2} \pi^1 \pi_{nb}^1 \pi^{*0} \delta^1 \delta_{nb}^1 \delta^{*1}$	4
	$\sigma^1 \sigma_{nb}^1 \sigma^{*1} \pi^1 \pi_{nb}^1 \pi^{*1} \delta^1 \delta_{nb}^1 \delta^{*1}$	6
	$\sigma^1 \sigma_{nb}^1 \sigma^{*1} \pi^1 \pi_{nb}^1 \pi^{*1} \delta^0 \delta_{nb}^1 \delta^{*2}$	3
S = 3/2	$\sigma^1 \sigma_{nb}^1 \sigma^{*1} \pi^1 \pi_{nb}^1 \pi^{*1} \delta^2 \delta_{nb}^1 \delta^{*0}$	2
	$\sigma^0 \sigma_{nb}^1 \sigma^{*2} \pi^1 \pi_{nb}^1 \pi^{*1} \delta^1 \delta_{nb}^1 \delta^{*1}$	2
	$\sigma^2 \sigma_{nb}^1 \sigma^{*0} \pi^1 \pi_{nb}^1 \pi^{*1} \delta^1 \delta_{nb}^1 \delta^{*1}$	2
	$\sigma^1 \sigma_{nb}^1 \sigma^{*1} \pi^0 \pi_{nb}^1 \pi^{*2} \delta^1 \delta_{nb}^1 \delta^{*1}$	2
	$\sigma^1 \sigma_{nb}^1 \sigma^{*2} \pi^1 \pi_{nb}^1 \pi^{*0} \delta^1 \delta_{nb}^1 \delta^{*1}$	1
	$\sigma^1 \sigma_{nb}^1 \sigma^{*1} \pi^1 \pi_{nb}^1 \pi^{*1} \delta^1 \delta_{nb}^1 \delta^{*1}$	2
	$\sigma^0 \sigma_{nb}^2 \sigma^{*1} \pi^1 \pi_{nb}^1 \pi^{*1} \delta^0 \delta_{nb}^2 \delta^{*1}$	2
	$\sigma^2 \sigma_{nb}^0 \sigma^{*1} \pi^1 \pi_{nb}^1 \pi^{*1} \delta^0 \delta_{nb}^2 \delta^{*1}$	2
S = 1/2	$\sigma^0 \sigma_{nb}^1 \sigma^{*2} \pi^1 \pi_{nb}^1 \pi^{*1} \delta^0 \delta_{nb}^1 \delta^{*2}$	1
	$\sigma^1 \sigma_{nb}^1 \sigma^{*1} \pi^2 \pi_{nb}^0 \pi^{*1} \delta^0 \delta_{nb}^2 \delta^{*1}$	1
	$\sigma^1 \sigma_{nb}^1 \sigma^{*1} \pi^0 \pi_{nb}^2 \pi^{*1} \delta^0 \delta_{nb}^2 \delta^{*1}$	1
	$\sigma^0 \sigma_{nb}^2 \sigma^{*1} \pi^1 \pi_{nb}^1 \pi^{*0} \delta^2 \delta_{nb}^0 \delta^{*1}$	1

We then extended the active space to include the three 2p orbitals and the associated six electrons on the central oxygen atom, producing a CAS(15,12) space. However, these extra three orbitals remain fully occupied in the ground-state wavefunction, and their inclusion has no effect on the relative energies as shown in the main text. The extra six orbitals are shown in Figure S10.

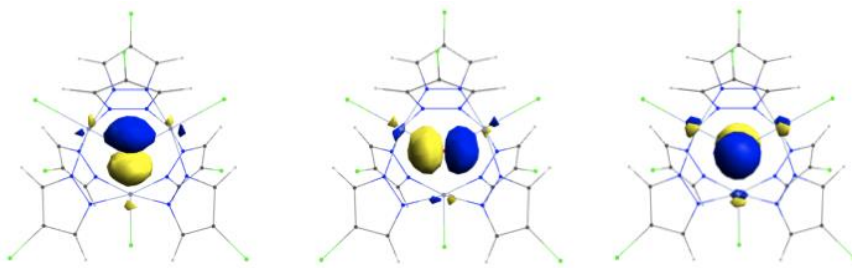


Figure S10. Op orbitals of the CAS(15,12) active space of the $\mathbf{1}^{\text{-}}$ molecule.

Table S5: NEV-PT2 energy and relative energies of different spin multiplicities of $\mathbf{1}^{\text{-}}$ and $\mathbf{1}^{\text{1-}}$ molecules

Multiplicity	Energy in eV	Relative energy in eV
$\mathbf{1}^{\text{-}}$		
10	-236394.780	0.016
8	-236394.778	0.018
6	-236394.790	0.005
4	-236394.794	0.002
2	-236394.796	0.000
$\mathbf{1}^{\text{1-}}$		
9	-236392.906	0.000
7	-236392.738	0.168
5	-236392.513	0.392
3	-236392.334	0.572
1	-236392.017	0.888

¹ F. Neese, *WIREs: Computational Molecular Science*, 2012, 2, 73-78.

² F. Neese, *WIREs Computational Molecular Science*, 2018, 8, e1327

³ J.P. Perdew, K. Burke and M. Ernzerhof, *Phys. Rev. Lett.* 1996, 77, 3865.

⁴ F. Weigend and R. Ahlrichs, *Phys. Chem. Chem. Phys.*, 2005, 7, 3297.

⁵ D. Andrae,U. Haeussermann, M. Dolg, H. Stoll, H. Preuss, *Theor. Chim. Acta*, 1990, 77, 123-141

⁶ S.M. Dancoff, *Phys. Rev.*, 1950, 78, 382.

⁷ P.J. Stephens, F.J. Devlin, C.F. Chabalowski and M.J. Frisch, *J. Phys. Chem.* 1994, 98, 11623-11627

⁸ T. Yanai, D. P. Tew, N. C. Handy, *Chem. Phys. Lett.*, 2004, 393, 51-57.

⁹ F. Weigend, *Phys. Chem. Chem. Phys.*, 2006, 8, 1057.

¹⁰ R. Izsák, F. Neese and W. Klopper , *J. Chem. Phys.*, 2013, 139, 094111.

¹¹ G. L. Stoychev, A. A. Auer, and F. Neese, *J. Chem. Theory Comput.*, 2017, 13, 554.